



Delft University of Technology

Lumped-element model for vortex–nozzle interaction in solid rocket motors

Hirschberg, L.; Hulshoff, S. J.

DOI

[10.2514/1.J058673](https://doi.org/10.2514/1.J058673)

Publication date

2020

Document Version

Final published version

Published in

AIAA Journal

Citation (APA)

Hirschberg, L., & Hulshoff, S. J. (2020). Lumped-element model for vortex–nozzle interaction in solid rocket motors. *AIAA Journal*, *58*(7), 3241-3244. <https://doi.org/10.2514/1.J058673>

Important note

To cite this publication, please use the final published version (if applicable). Please check the document version above.

Copyright

Other than for strictly personal use, it is not permitted to download, forward or distribute the text or part of it, without the consent of the author(s) and/or copyright holder(s), unless the work is under an open content license such as Creative Commons.

Takedown policy

Please contact us and provide details if you believe this document breaches copyrights. We will remove access to the work immediately and investigate your claim.



Technical Notes

Lumped-Element Model for Vortex–Nozzle Interaction in Solid Rocket Motors

L. Hirschberg*

DLR, German Aerospace Center, 10623 Berlin, Germany
and

S. J. Hulshoff†

Delft University of Technology,
2629 HS Delft, The Netherlands

<https://doi.org/10.2514/1.J058673>

Nomenclature

B	=	total enthalpy, $\text{m}^2 \cdot \text{s}^{-2}$
B_0	=	reference uniform observer state total enthalpy, $\text{m}^2 \cdot \text{s}^{-2}$
B'	=	total enthalpy fluctuation; $B - B_0$, $\text{m}^2 \cdot \text{s}^{-2}$
\tilde{B}'	=	dimensionless upstream acoustic response; $2B'/U^2$
c	=	local speed of sound, $\text{m} \cdot \text{s}^{-1}$
L_{eff}	=	effective length; $(V_{\text{residual}} + V_c)/(4S_1^2)$, m
\tilde{L}_{eff}	=	dimensionless effective length; L_{eff}/S_1
M	=	upstream Mach number; $M \equiv U/c$
R_Γ	=	vortex-core radius, m
S_1	=	upstream half-channel height measured with respect to the symmetry axis, m
S_2	=	nozzle throat half-height, m
t	=	time, s
t_{emission}	=	emission time; $t + x_{\text{observer}}/(c - U)$, s
\tilde{t}	=	dimensionless time; tU/S_1
$\tilde{t}_{\text{emission}}$	=	dimensionless emission time; $t_{\text{emission}}U/S_1$
U	=	average upstream flow speed, $\text{m} \cdot \text{s}^{-1}$
U	=	average upstream flow velocity, $\text{m} \cdot \text{s}^{-1}$
V_c	=	nozzle cavity volume, m^3
V_{residual}	=	volume accounting for residual local compressibility, namely, when $V_c = 0$, m^3
\mathbf{v}	=	local velocity; $u_i \mathbf{e}_i$, $\text{m} \cdot \text{s}^{-1}$
x	=	spatial coordinate, m
x_{observer}	=	observer position, m
\tilde{x}	=	dimensionless spatial coordinate; x/S_1
$\tilde{x}_{\text{observer}}$	=	dimensionless observer position; x_{observer}/S_1
Γ	=	vortex circulation, $\text{m}^2 \cdot \text{s}^{-1}$
$\tilde{\Gamma}$	=	dimensionless vortex circulation; $\Gamma/(US_1)$
$\Delta B'$	=	vortex–nozzle interaction source pulse, $\text{m}^2 \cdot \text{s}^{-2}$
$\Delta \tilde{B}'$	=	dimensionless vortex–nozzle interaction source pulse; $2\Delta B'/U^2$
Δ_{peak}	=	relative difference in peak values of scaled upstream acoustic response
τ	=	pulse-width-fit parameter
$\tau/2$	=	vortex–nozzle interaction pulse width, s

$\tilde{\tau}/2$ = dimensionless pulse width; $U\tau/(2S_1)$
 ω_z = normal vorticity component, s^{-1}

I. Introduction

S ELF-SUSTAINED limit-cycle pressure pulsations in solid rocket motors (SRMs) are a well-documented problem [1–10]. SRMs are essentially a long tube closed at the head end and with a nozzle at the tail end. The walls are covered by a layer of solid propellant, which is often manufactured in annular segments. In Ariane 5 P230 SRMs, these segments are separated by thermal inhibitors. After ignition, combustion of the propellant occurs in a surface flame on its exposed surface. The combustion process causes an injection of gas into the combustion chamber, which establishes a choked nozzle flow.

Small tactical SRMs can display high-amplitude pulsations of $p'/p = \mathcal{O}(10^{-1})$ resulting from a feedback loop established through a pressure coupling of the flame on the surface of the propellant and a longitudinal acoustic standing wave. A limit-cycle amplitude is then reached due to shockwave dissipation [1–3]. In the literature, authors propose one-dimensional (1-D) models for limit-cycle amplitude prediction [2,3]. The combustion chamber is typically an order of magnitude longer than its diameter. As the oscillations are driven by the first or second longitudinal acoustic mode, the oscillation frequency is far below the cutoff for transversal modes. Hence, the acoustic field is uniform over the cross section of the chamber, allowing a global 1-D acoustical model to be used. One-dimensional models are particularly attractive because they allow for efficient parametric studies without being computationally expensive.

Large SRMs (e.g., P230 or Titan 4 Solid Rocket Motor Upgrade (SRMU)) display pulsations in the moderate-amplitude regime $p'/p = \mathcal{O}(10^{-3})$ [4–9]. In these systems, saturation of the limit cycle is due to the formation of discrete coherent vortical structures, referred to as vortices. These are formed upstream from the nozzle, where neighboring annular solid propellant segments meet, due to a hydrodynamic instability triggered by acoustic perturbations. The uniform (1-D) acoustic perturbation in a cross section implies that axisymmetric vortices are formed. The vortices convect downstream, where they produce sound through interaction with the choked nozzle as they exit the combustion chamber. This mechanism is referred to as vortex–nozzle interaction [4,5,7,9–13]. Vortex–nozzle interaction leads to the establishment of an acoustic standing wave, which provides the acoustic perturbations establishing a feedback loop [5–11].

For vortex-driven self-sustained pressure pulsations, the presence of a cavity around the nozzle inlet (as in integrated nozzles) is known to have a major influence [5,7,9,10]. Indeed, cold-gas scale experiments of the Ariane 5 P230 SRM show that the limit-cycle amplitude of vortex-driven self-sustained pressure pulsations is proportional to the nozzle cavity volume V_c [7,9]. In real systems, the cavity appears after partial combustion of the propellant surrounding the inlet of the integrated nozzle used in most SRMs. In Refs. [4,5,11,12], the importance of V_c for vortex-driven pulsations is confirmed and analyzed. The cavity is formed by combustion of the propellant around the integrated nozzle. The evolution in time of this cavity is predicted by standard combustion models used to predict the performance of the SRM [14].

Efficient 1-D models would be valuable engineering tools in the design process of large SRMs. Ferretti et al. [15] made a first step in the development of such 1-D models. However, the model presented in Ref. [15] cannot describe the influence of V_c . In particular, in Ref. [15], production of sound is assumed to be due to the variation (gradient) of the cross section (at the nozzle of the SRM) but no discernible physical justification is provided for the approach. The presence of a nozzle

Received 11 June 2019; revision received 3 April 2020; accepted for publication 11 May 2020; published online 26 May 2020. Copyright © 2020 by the American Institute of Aeronautics and Astronautics, Inc. All rights reserved. All requests for copying and permission to reprint should be submitted to CCC at www.copyright.com; employ the eISSN 1533-385X to initiate your request. See also AIAA Rights and Permissions www.aiaa.org/randp.

*DLR-DAAD Postdoctoral Fellow, Institute of Propulsion Technology, Engine Acoustics; lionel.hirschberg@dlr.de. Member AIAA.

†Assistant Professor, Faculty of Aerospace Engineering.

cavity inlet (viz., the absence of a single valued cross-sectional area) would imply the introduction of a singularity in this modeling approach.

Thus, to develop a 1-D model for limit-cycle amplitude prediction for these large SRMs, it is first necessary to develop a vortex–nozzle interaction sound source model that can take into account the effect of V_c . In this Note, the most elementary version of such a model, based on a scaling rule derived from systematic numerical simulations of vortex–nozzle interaction (Sec. II), is proposed (Sec. III).

II. Euler-Model Simulations-Based Scaling Rule

Inspired by Hulshoff et al. [13], systematic two-dimensional planar numerical simulations of vortex–nozzle interaction as an indirect sound source have been undertaken [4,11,12]. These were carried out using a two-dimensional (2-D) Euler model [4,11–13], which solves the compressible frictionless governing Euler equations. In SRMs, vortices are formed close to the exposed surface of the propellant, i.e., close to the wall of the combustion chamber [7,10]. Since the dynamics of the vortices and sound production are strongly influenced by the walls [4,5], one expects that a 2-D planar model provides at least qualitative insight into vortex–nozzle interaction. Two-dimensional vortex–nozzle interaction modeling approaches have been successful in the past [5,9]. In particular, by using a 2-D vortex–nozzle interaction approach, Hirschberg et al. [5] were able to predict pulsations amplitudes in a cold-gas experiment within a factor two. In Refs. [4,12], one finds details on the equations solved by Euler model, the numerical integration methods used, how vortex–nozzle simulations were carried out including the upstream vortex generation process, and grid studies that have been performed.

Two nozzle inlet geometries were considered. Figure 1a shows the first: an integrated nozzle geometry with a cavity surrounding its inlet. Figure 1b shows the second: a nozzle with the inlet forming a right angle corner with the combustion chamber sidewall. The vorticity distribution field [obtained with $M = 0.20$, $\tilde{\Gamma} = -0.1$, $h/S_1 = 0.4$, $S_1/S_2 = 3$, $R_\Gamma/S_1 = 0.3$, and $V_c/(4S_1^3) = 0.7$] with an approaching vortex upstream from the nozzle are shown both for the case with a nozzle cavity (Fig. 1a) and without a nozzle cavity (Fig. 1b). One observes a thin layer of vorticity that develops from the sharp leading edge of the nozzle cavity inlet. Its presence does not contribute to the production of sound. The cavity volume V_c is taken to be the volume of an upstream duct segment of length $0.7S_1$, which is representative of an Ariane 5 SRM during flight [5,7]. In both cold-gas scale experiments [7,9] and scale experiments with combustion [10], the configuration without a nozzle cavity did not display self-sustained pulsations.

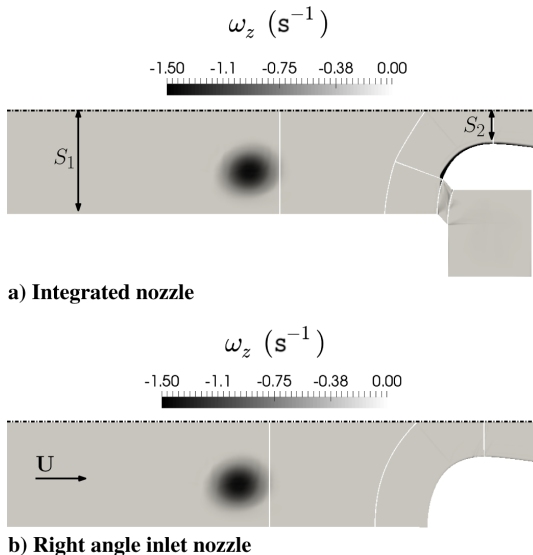


Fig. 1 Nozzle inlet geometries for a nozzle inlet Mach number of $M = 0.20$ a) with nozzle cavity and b) without. Grayscale is for the normal vorticity component ω_z .

The upstream release height h measured from the lower upstream channel wall to the center of the vortex was varied in the range $0.4 \leq h/S_1 \leq 0.6$. The upstream Mach number was varied in the range typical for SRMs: $0.05 \leq M \leq 0.2$ [7]. Vortices with vortex-core radii in the range $0.3 \leq R_\Gamma/S_1 \leq 0.4$ and with dimensionless vortex circulation $\tilde{\Gamma} \equiv \Gamma/(S_1 U)$ in the range $0.1 \leq |\tilde{\Gamma}| \leq 1$ were used.

These parameter studies led to the development of a scaling rule for the dimensionless upstream acoustic response due to vortex–nozzle interaction $\tilde{B}' \equiv 2B'/U^2$ [4,11]:

$$\tilde{B}' \propto \tilde{\Gamma} \tilde{M} \tilde{L}_{\text{eff}} \quad (1)$$

where $\tilde{L}_{\text{eff}} \equiv L_{\text{eff}}/S_1 = (V_c + V_{\text{residual}})/(4S_1^3)$ is the dimensionless effective length. The linear dependence on \tilde{L}_{eff} can be explained as being due to the compressibility of the gas in the cavity. The dimensions of the cavity are small compared to the typical acoustic wavelength of the waves. This compressibility effect results into an acoustic velocity perturbation normal to the vortex path. Vortex sound theory [16] explains that this results into sound-wave generation. Furthermore, a linear dependence on the upstream Mach number M and the dimensionless vortex circulation $\tilde{\Gamma}$ was found [4,11]. Importantly, these investigations identified parameters that do not significantly influence the upstream acoustic response due to vortex–nozzle interaction, viz., the vortex-core radius R_Γ and the upstream release height h of the vortex measured from the upstream-lower-channel wall to the center of the vortex.

Vortex–nozzle interaction simulations with and without the presence of a nozzle cavity showed that one can take into account residual compressibility effects, when $V_c = 0$, with a volume V_{residual} (i.e., V_{residual} accounts for local compressibility even in absence of a nozzle cavity [4]). In Ref. [4], an analysis is provided that shows that $V_{\text{residual}}/(4S_1^3) \approx 0.2$. In Eq. (1), the sum $V_{\text{residual}} + V_c$ is scaled by $4S_1^3$: a S_1 long section of the upstream channel [4]. In Refs. [4,11], it is reported that, for $|\tilde{\Gamma}| \gg 1$, the upstream acoustic response becomes proportional to $\tilde{\Gamma}^2$ and is dominated by convective radiation effects at the nozzle. However, as the estimated range of vortex circulation is $0.1 < \tilde{\Gamma} < 1$ [4,11], these effects are negligible compared to local compressibility effects that are linear in $\tilde{\Gamma}$.

III. Vortex–Nozzle Interaction Lumped-Element Model

In the following, a brief description of a 1-D lumped-element vortex–nozzle interaction sound source model is provided. To obtain analytical results, it is assumed that the choked nozzle acts acoustically as a closed wall. A dimensionless dipolar source $\Delta\tilde{B}'(\tilde{x} = 0, \tilde{t})$, with dimensionless spatial coordinate $\tilde{x} \equiv x/S_1$ and time $\tilde{t} \equiv tU/S_1$, is placed at a dimensionless distance \tilde{L}_{eff} from a perfectly reflecting acoustic wall (dashed vertical line in Fig. 2). Initially, two acoustic plane waves traveling in opposite directions emanate from the source: upstream $-\Delta\tilde{B}'(\tilde{t} + M\tilde{x}/(1-M))/2$ and downstream $\Delta\tilde{B}'(\tilde{t} - M\tilde{x}/(1+M))/2$ (Fig. 2a). The initially right-traveling plane wave is reflected against the wall, resulting in a left-traveling plane wave

$$\Delta\tilde{B}'(\tilde{t} + M(\tilde{x}/(1-M) - 2\tilde{L}_{\text{eff}}/(1-M^2)))/2$$

Thus, as can be seen in Fig. 2b, the acoustic field for an upstream observer at distance $\tilde{x}_{\text{observer}} < 0$ from the source is

$$\begin{aligned} \tilde{B}'(\tilde{x}_{\text{observer}}, \tilde{t}) &= -\frac{1}{2} \left(\Delta\tilde{B}' \left(\tilde{t} + \frac{M\tilde{x}_{\text{observer}}}{1-M} \right) \right. \\ &\quad \left. - \Delta\tilde{B}' \left(\tilde{t} + M \left(\frac{\tilde{x}_{\text{observer}}}{1-M} - \frac{2\tilde{L}_{\text{eff}}}{1-M^2} \right) \right) \right) \\ &\approx -\frac{M\tilde{L}_{\text{eff}}}{1-M^2} \left(\frac{d\Delta\tilde{B}'}{d\tilde{t}} \right)_{\tilde{t}_{\text{emission}}} \end{aligned} \quad (2)$$

where $\tilde{t}_{\text{emission}} = \tilde{t} + M\tilde{x}_{\text{observer}}/(1-M)$. Making a low-Mach-number approximation ($M^2 \ll 1$), Eq. (2) becomes

$$\tilde{B}'(\tilde{x}_{\text{observer}}, \tilde{t}) = -M\tilde{L}_{\text{eff}} \left(\frac{d\Delta\tilde{B}'}{d\tilde{t}} \right)_{\tilde{t}_{\text{emission}}} \quad (3)$$

Taking into account the $\tilde{\Gamma}$ proportionality in Eq. (1), the source $\Delta\tilde{B}'(\tilde{x} = 0, \tilde{t})$ is prescribed as follows:

$$\Delta\tilde{B}'(\tilde{x} = 0, \tilde{t}) = \begin{cases} \tilde{\Gamma}\kappa \left(\frac{4\tilde{t}}{\tilde{\tau}} \right)^l \sin^2 \left(\frac{2\pi}{\tilde{\tau}} \tilde{t} \right) & \text{for } 0 \leq \tilde{t} \leq \tilde{\tau}/2 \\ 0 & \text{for all other } \tilde{t} \end{cases} \quad (4)$$

where κ , l , and $\tilde{\tau}$ are fit parameters. Substitution in Eq. (3) yields

$$\tilde{B}'(\tilde{x}_{\text{observer}}, \tilde{t}) = \begin{cases} -\tilde{\Gamma}M\tilde{L}_{\text{eff}} \frac{d}{d\tilde{t}} \left(\kappa \left(\frac{4\tilde{t}_{\text{emission}}}{\tilde{\tau}} \right)^l \sin^2 \left(\frac{2\pi}{\tilde{\tau}} \tilde{t}_{\text{emission}} \right) \right) & \text{for } 0 \leq \tilde{t}_{\text{emission}} \leq \tilde{\tau}/2 \\ 0 & \text{for all other } \tilde{t}_{\text{emission}} \end{cases} \quad (5)$$

which has the same $\tilde{\Gamma}M\tilde{L}_{\text{eff}}$ proportionality as Eq. (1).

The values of κ , l , and $\tilde{\tau}$ were chosen based on a visual fit of a single Euler-model result obtained for $M = 0.058$, $\tilde{\Gamma} = -0.9$, $h/S_1 = 0.4$, and $R_\Gamma/S_1 = 0.3$; as shown in Fig. 3, this yields $\kappa = 1.35$, $l = 2$, and $\tilde{\tau} = 4.07$. Care was taken to accurately fit the peak value of the scaled Euler-model upstream acoustic response $\tilde{B}'_{\text{peak,Euler}}/(\tilde{\Gamma}M\tilde{L}_{\text{eff}})$, resulting in $\tilde{B}'_{\text{peak,lumped}}/(\tilde{\Gamma}M\tilde{L}_{\text{eff}}) = 3.943$.

Using this set of fit parameters, the lumped-element model compares fairly well with Euler-model results obtained using different values of driving parameters. For quantitative comparison, consult Table 1, where

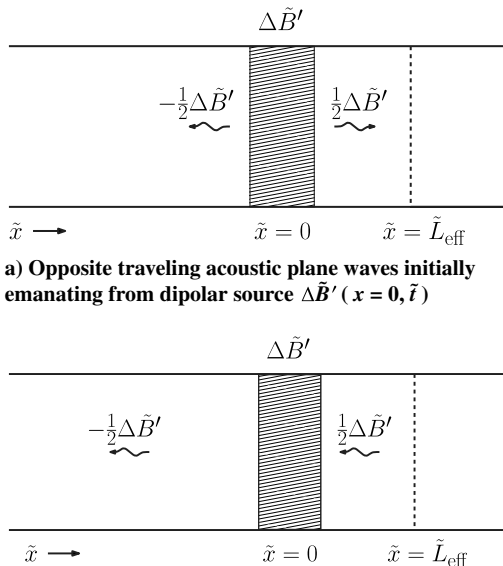


Fig. 2 Sketch of vortex–nozzle interaction lumped-element model.

$$\Delta_{\text{peak}} \equiv \frac{|\tilde{B}'_{\text{peak,lumped}}/(\tilde{\Gamma}M\tilde{L}_{\text{eff}}) - \tilde{B}'_{\text{peak,Euler}}/(\tilde{\Gamma}M\tilde{L}_{\text{eff}})|}{|\tilde{B}'_{\text{peak,lumped}}/(\tilde{\Gamma}M\tilde{L}_{\text{eff}})|} \quad (6)$$

is the relative difference in scaled upstream acoustic response peak between the lumped model and the Euler model. The Euler-model results in Table 1 are for $h/S_1 = 0.4$ and $R_\Gamma/S_1 = 0.3$. Note that h/S_1 and R_Γ/S_1 do not significantly influence the results of the Euler model [4,11]. One finds that, overall, positive peak values of the dimensionless acoustic response are reproduced within 24% when compared to a set of Euler-model results obtained for parameters in the following ranges: $0.05 \leq M \leq 0.2$, $0.1 \leq |\tilde{\Gamma}| \leq 1$, $0.3 \leq R_\Gamma/S_1 \leq 0.4$, and $0.4 \leq h/S_1 \leq 0.6$.

In Fig. 3 and other results provided in Ref. [4], around $\tilde{t}_{\text{emission}} \simeq 2$, just after the strongly positive peak, one observes a decaying oscillation in the numerical simulation results. This decaying oscillation

corresponds either to the second transversal channel-cavity mode [4] or a Helmholtz resonance, which becomes more pronounced as the upstream Mach number is increased. This effect is not reproduced in the presently proposed lumped-element model, which is 1-D.

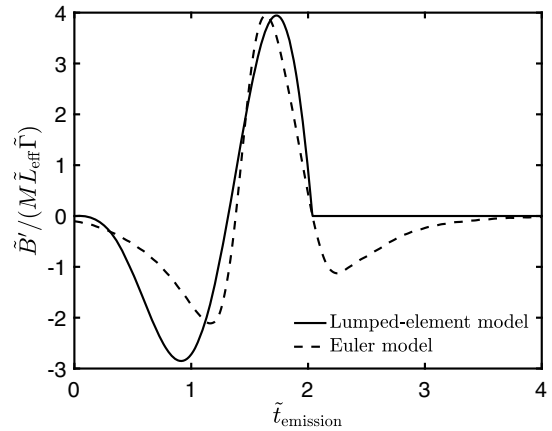


Fig. 3 Lumped-element model visual fit to Euler-model result for $M = 0.058$, $\tilde{\Gamma} = -0.9$, $R_\Gamma/S_1 = 0.3$, $h/S_1 = 0.4$, and $\tilde{L}_{\text{eff}} = 0.9$: yields $\kappa = 1.35$, $l = 2$, and $\tilde{\tau} = 4.07$.

Table 1 Maximum peak value deviation Δ_{peak} between lumped-element model and Euler model

\tilde{L}_{eff}	M	$\tilde{\Gamma}$	$\tilde{B}'_{\text{peak,Euler}}/(\tilde{\Gamma}M\tilde{L}_{\text{eff}})$	$\Delta_{\text{peak}} \%$
0.90	0.058	-0.90	—	—
0.90	0.097	-0.90	4.877	24
0.90	0.097	-0.10	3.839	3
0.90	0.20	-0.10	4.371	11
0.90	0.20	-0.90	4.152	5
0.20	0.097	-0.10	3.462	12
0.20	0.20	-0.10	4.225	7

The source model described by Eq. (2) could be implemented in a more complex acoustical model including Helmholtz resonance of the cavity. In such a model, acoustical nozzle-radiation losses, not modeled in the present work, could also be taken into account.

IV. Conclusions

A straightforward one-dimensional lumped-element model for the vortex–nozzle interaction sound source, based on systematic numerical simulations, is proposed. A key feature of this model is that it only concerns the production of sound due to the interaction of a fully mature vortex with a choked nozzle. This model captures the most important features of the upstream acoustic response due to vortex–nozzle interaction, which are due to local compressibility of the fluid in the nozzle cavity and around the nozzle inlet. It can be implemented in a one-dimensional model to simulate the influence of different design parameters on vortex-driven pulsation amplitudes. However, to do this, one should develop a vortex formation and convection model, which would be determined by key geometric features of the combustion chamber.

Acknowledgments

This Note was written while Lionel Hirschberg was the beneficiary of a Deutsches Zentrum für Luft- und Raumfahrt (DLR) Deutscher Akademischer Austauschdienst (DAAD) postdoctoral fellowship (no. 57424730). The authors thank Yves Aurégan for an insightful discussion about the possible occurrence of a Helmholtz resonance in the results of the numerical investigations. Thanks to Thierry Schuller, Christophe Schram, Friedrich Bake, Karsten Knobloch, and Lars Enghardt for their support.

References

- [1] Flandro, G. A., Fischbach, S. R., and Majdalani, J., “Nonlinear Rocket Motor Stability Prediction: Limit Amplitude, Triggering, and Mean Pressure Shift,” *Physics of Fluids*, Vol. 19, No. 9, 2007, Paper 094101. <https://doi.org/10.1063/1.2746042>
- [2] Levine, J. N., and Baum, J. D., “Modeling of Nonlinear Combustion Instability in Solid Propellant Rocket Motors,” *Symposium (International) on Combustion*, Vol. 19, No. 1, 1982, pp. 769–776. [https://doi.org/10.1016/S0082-0784\(82\)80252-X](https://doi.org/10.1016/S0082-0784(82)80252-X)
- [3] Greatrix, D. R., “Scale Effects on Solid Rocket Combustion Instability Behaviour,” *Energies*, Vol. 4, No. 1, 2011, pp. 90–107. <https://doi.org/10.3390/en4010090>
- [4] Hirschberg, L., “Low Order Modeling of Vortex Driven Self-Sustained Pressure Pulsations in Solid Rocket Motors,” Ph.D. Thesis, Centrale Supélec, Univ. of Paris-Saclay, France, 2019.
- [5] Hirschberg, L., Schuller, T., Collinet, J., Schram, C., and Hirschberg, A., “Analytical Model for the Prediction of Pulsations in a Cold-Gas Scale-Model of a Solid Rocket Motor,” *Journal of Sound and Vibration*, Vol. 19, April 2018, pp. 445–368. <https://doi.org/10.1016/j.jsv.2018.01.025>
- [6] Dotsion, K. W., Koshigoe, S., and Pace, K. K., “Vortex Shedding in a Large Solid Rocket Motor Without Inhibitors at the Segmented Interfaces,” *Journal of Propulsion and Power*, Vol. 13, No. 2, 1997, pp. 197–206. <https://doi.org/10.2514/2.5170>
- [7] Anthoine, J., “Experimental and Numerical Study of Aeroacoustic Phenomena in Large Solid Propellant Boosters, with application to the Ariane 5 Solid Rocket Motor,” Ph.D. Thesis, Free Univ. of Brussels, Brussels, Belgium, 2000.
- [8] Fabignon, Y., Dupays, J., Avalon, G., Vuillot, F., Lupoglazoff, N., Casalis, G., and Prévost, M., “Instabilities and Pressure Oscillations in Solid Rocket Motors,” *Aerospace Science and Technology*, Vol. 7, No. 3, 2003, pp. 191–200. [https://doi.org/10.1016/S1270-9638\(02\)01194-X](https://doi.org/10.1016/S1270-9638(02)01194-X)
- [9] Anthoine, J., Buchlin, J.-M., and Hirschberg, A., “Effect of Nozzle Cavity on Resonance in Large SRM: Theoretical Modeling,” *Journal of Propulsion and Power*, Vol. 18, No. 2, 2002, pp. 304–311. <https://doi.org/10.2514/2.5935>
- [10] Gallier, S., Prevost, M., and Hijlkema, J., “Effects of Cavity on Thrust Oscillations in Subscale Solid Rocket Motors,” *45th AIAA/ASME/ASEE Joint Propulsion Conference & Exhibit*, AIAA Paper 2009-5253, Aug. 2009. <https://doi.org/10.2514/6.2009-5253>
- [11] Hirschberg, L., Hulshoff, S. J., Collinet, J., Schram, C., and Schuller, T., “Vortex Nozzle Interaction in Solid Rocket Motors: A Scaling Law for Upstream Acoustic Response,” *Journal of the Acoustical Society of America*, Vol. 144, No. 1, 2018, pp. EL46–EL51. <https://doi.org/10.1121/1.5046441>
- [12] Hirschberg, L., Hulshoff, S. J., Collinet, J., Schram, C., and Schuller, T., “Influence of Nozzle Cavity on Indirect Vortex- and Entropy-Sound Production,” *AIAA Journal*, Vol. 57, No. 7, March 2019, pp. 3100–3103. <https://doi.org/10.2514/1.J058138>
- [13] Hulshoff, S. J., Hirschberg, A., and Hofmans, G. C. J., “Sound Production of Vortex Nozzle Interactions,” *Journal of Fluid Mechanics*, Vol. 439, July 2001, pp. 335–352. <https://doi.org/10.1017/S0022112001004554>
- [14] Cavalli, E., “Modeling and Numerical Simulation of Solid Rocket Motors Internal Ballistics,” Ph.D. Thesis, Univ. of Rome “La Sapienza,” Rome, Italy, 2009.
- [15] Ferretti, V., Favini, B., Cavallini, E., Serraglia, F., and Di Giacinto, M., “Vortex-Sound Generated Pressure Oscillations Simulation in Internal Flow by Means of Q-1D Model,” *4th European Conference for Aerospace Sciences*, EUCASS, St. Petersburg, Russia, July 2011, pp. 1–15.
- [16] Howe, M. S., “The Dissipation of Sound at an Edge,” *Journal of Sound and Vibration*, Vol. 70, No. 3, 1980, pp. 407–411. [https://doi.org/10.1016/0022-460X\(80\)90308-9](https://doi.org/10.1016/0022-460X(80)90308-9)

D. S. Stewart
Associate Editor